Geotextiles and Geomembranes 12 (1993) 327–349

Interaction between Cohesive-Frictional Soil and Various Grid Reinforcements

D. T. Bergado, J. C. Chai, H. O. Abiera, M. C. Alfaro & A. S. Balasubramaniam

Asian Institute of Technology, GPO Box 2754, Bangkok, Thailand

(Received 3 March 1992; accepted 15 July 1992)

ABSTRACT

A total of 52 large-scale laboratory pullout and 24 large-scale direct-shear tests were conducted to investigate the interaction behavior between the different reinforcements and cohesive-frictional soil. The reinforcements used were steel grids, bamboo grids, and polymer geogrids. The backfill material used was locally available weathered Bangkok clay. The test results show that the inextensible reinforcements, such as steel grids, move approximately as a rigid body during the pullout test, and the maximum pullout resistance was reached within a relatively small pullout displacement. For extensible reinforcements, such as Tensar geogrids, the degree of resistance mobilization along the reinforcement varies, and the pullout-resistance achieved in the tests was controlled by the stiffness of the reinforcement. For steel grids, the friction resistance from the longitudinal member contributed only to about 10% of the total pullout resistance of the grids. The pullout of the bamboo and Tensar geogrids without transverse members yields 80–90% of the pullout resistance of the corresponding grids with transverse members, attributed to the nodes or ribs on longitudinal members. The bond coefficient as calculated for steel and bamboo grids demonstrated that the steel grids yielded a higher bond coefficient than that of the bamboo grids with the same grid size. However, for a polymer geogrid, the bond coefficient cannot be calculated from a pullout test because of the complicated pullout-resistance-mobilization mechanism along the reinforcement. The large-scale direct-shear-test results showed that, for the soil/grid-reinforcement interfaces, shear resistance can exceed the direct-shear resistance of the soil itself owing to the influence of the apertures on the

Geotextiles and Geomembranes 0266–1144/93/$06·00

grids. Finally, for compacted weathered clay, the strength parameters obtained from large-scale direct-shear tests were found to be substantially smaller than the results of triaxial UU tests. This may be because the failure plane in the large-scale direct-shear test was formed progressively, and the peak soil strength along the predetermined shear plane may not have been mobilized simultaneously.

NOTATION

A Total shear area
B Cohesion
D Thickness of the bearing member
N_c, N_q Bearing-capacity factors
S Space between two neighboring transverse members
α_{ds} Ratio of reinforcement shear area to total shear area
δ Skin-friction angle
σ_b Bearing resistance on grid-bearing member
σ_n Normal stress at shear plane
ϕ Friction angle of soil from triaxial test
ϕ_{ds} Friction angle of soil from direct-shear test

1 INTRODUCTION

For the last two decades, the practice of reinforcing the soil with tensile inclusions has been widely implemented in geotechnical engineering. Several types of materials have been used as soil reinforcements, namely: steel strips, geotextiles, polymer geogrids, steel grids, and bamboo grids. Different reinforcements can be economically used for different purpose, e.g. the locally available bamboo can be effectively used to reinforce the embedment constructed on soft ground because the reinforcement force is needed only during and immediately after construction.

At an early stage of the earth-reinforcement technique, from most case histories, the backfill materials used were frictional materials. Recently, because of cost considerations, locally available and poor-quality backfills have been successfully used, such as the test reinforced wall/embankment constructed in the campus of the Asian Institute of Technology (Bergado *et al.*, 1991).

Whatever reinforcement and backfill materials are used for the design of an earth-reinforcement system, the reinforcement/backfill-soil interaction

properties play an important role. The interaction mechanism between the reinforcement and the soil can be simply classified into two types, namely: soil sliding in direct shear over the reinforcement and pullout of reinforcement from the soil (Jewell *et al.*, 1984). Thus the direct-shear and pullout tests are widely used methods to study quantitatively these interaction mechanisms.

In this study, large laboratory direct-shear and pullout tests were used to investigate the shear resistance and bond coefficient of various reinforcements embedded in weathered Bangkok clay, which is the most abundant and least expensive backfill material for reinforced-earth construction in the Bangkok area. Three types of reinforcement were used, namely: steel grids, polymer geogrids and bamboo grids. The study focused on the comparison of the direct-shear and pullout resistances for the different types of reinforcement, and the comparison of the pullout resistance of the reinforcement with or without transverse members. The tests were interpreted in terms of total-stress strength parameters.

2 THEORETICAL BACKGROUND

The reinforcements can be divided into three groups, namely: (i) sheet reinforcements; (ii) strip reinforcements, and (iii) grid reinforcements. For sheet- and strip-type reinforcements, the soil/reinforcement interactions are controlled by friction between the soil and the reinforcement. However, for grid reinforcements, the direct-shear interaction mode is controlled not only by the friction between the soil and the grid surface area but also by the friction of the soil itself. The pullout resistance is governed by the friction between the soil and the grid surface as well as the bearing resistance of the soil on the transverse members of grid. Usually, the bearing resistance is much higher than the friction resistance (Chang *et al.*, 1977).

2.1 Direct-shear resistance

The direct-shear resistance between the reinforcement and the soil has two components, namely: the shear resistance between the soil and the reinforcement-plane surface area, and the soil-to-soil shear resistance at the grid opening (Jewell *et al.*, 1984). The direct-shear resistance, P_s, can be expressed as follows:

$$P_s = \sigma_n A[\alpha_{ds} \tan (\delta + (1 - \alpha_{ds})\tan \phi_{ds})] \quad (1)$$

where ϕ_{ds} is the friction angle of soil in direct shear, δ is the skin-friction angle between soil and reinforcement shear surface, α_{ds} is the ratio between the reinforcement shear area and the total shear area, σ_n is the normal stress at the shear plane, and A is the total shear area.

2.2 Pullout resistance

Generally, the pullout resistance consists of two parts, namely: friction resistance and passive-bearing resistance. The friction resistance can be calculated from eqn (1) by using the reinforcement frictional area, A and putting α_{ds} equal to 1·0.

The passive-bearing resistance is evaluated by bearing-capacity theory and can be expressed as follows:

$$\sigma_b = CN_c + \alpha_n N_q \tag{2}$$

where σ_b is the bearing resistance on grid-bearing members, C is the cohesion of backfill soil σ_n is the applied normal pressure at the soil/reinforcement interface, and N_c and N_q are the bearing-capacity factors. Different assumptions have been used for determining the bearing-capacity factors. Peterson and Anderson (1980) assumed a normal characteristic field for a foundation rotated to the horizontal as shown in Fig. 1(a). The expressions for N_q and N_c are as follows:

$$N_q = \exp[\pi \tan \phi]\tan^2\left(\frac{\pi}{4} + \frac{\phi}{2}\right) \tag{3}$$

$$N_c = (N_q - 1)\cot \phi \tag{4}$$

where ϕ is the friction angle of the soil.

Jewell *et al.* (1984) assumed a punching-failure mode for reinforcement passive-bearing resistance. The stress characteristic field is as shown in Fig. 1(b). The expressions for bearing-capacity factors are:

$$N_q = \exp[\pi/2 + \phi)\tan \phi]\tan\left(\frac{\pi}{4} + \frac{\phi}{2}\right) \tag{5}$$

$$N_c = (N_q - 1)\cot \phi \tag{4a}$$

Equations (3) and (4) and (5) and (4*a*) form the apparent upper and lower bounds of pullout passive-bearing resistance.

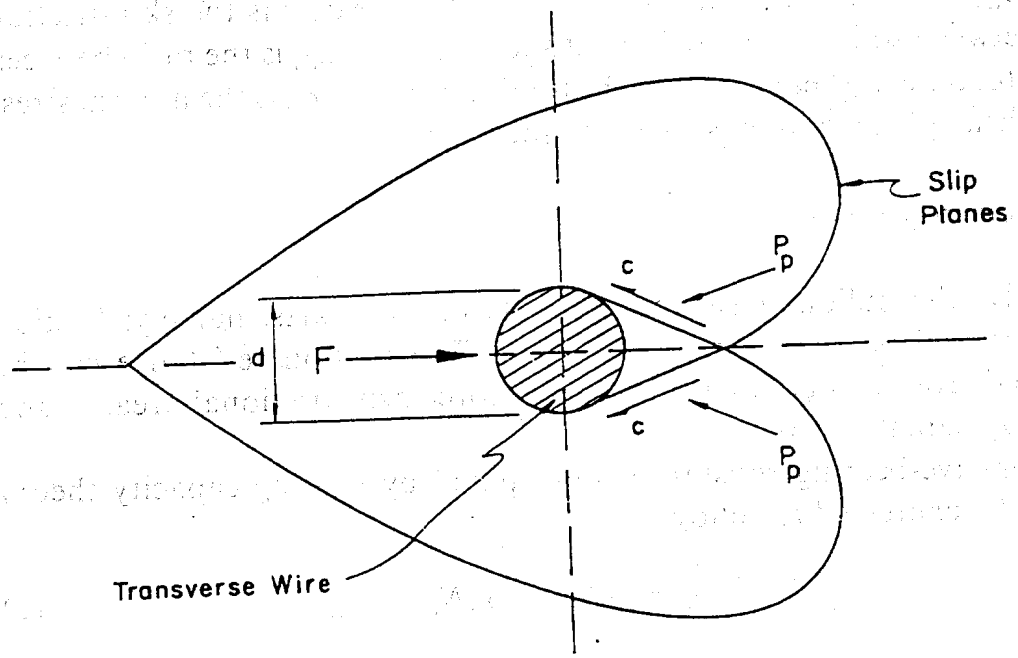

$$N_q = e^{(\pi \tan \phi)} \tan^2 (45 + \phi/2)$$

Bearing Capacity Failure (After Peterson & Anderson, 1980)

(a)

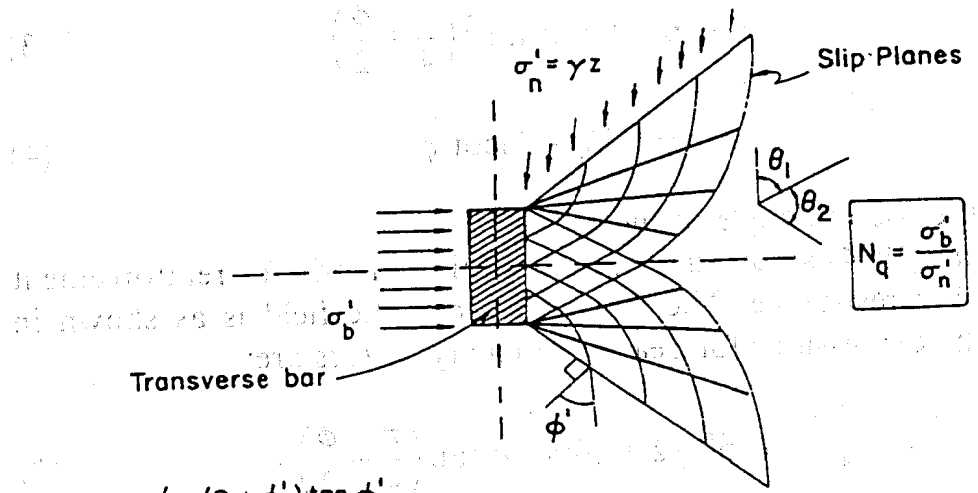

$$N_q = e^{(\pi/2 + \phi') \tan \phi'} \tan (45 + \phi'/2)$$

Punching Shear Failure (After Jewell et al, 1984)

(b)

Fig. 1. Passive-bearing failure mechanisms: (a) general shear; (b) punching shear.

2.3 Bond coefficient

The bond coefficient between the reinforcement and soil is defined as follows:

$$\text{bond coefficient} = \frac{\text{resistance between soil and reinforcement}}{\text{resistance between soil and soil}} \quad (6)$$

For the soil/reinforcement direct-shear-interaction mechanism, the resistance between soil and soil is the direct-shear resistance of the soil with the same shear area as that of the soil/reinforcement interface, whereas, for the soil/reinforcement pullout-interaction mechanism, the soil-to-soil resistance is the direct-shear resistance of the soil with a shear area equivalent to the total interface areas above and below the reinforcement.

3 LABORATORY TEST PROGRAM

In all, 52 pullout tests and 24 large-scale direct-shear tests were conducted in this study (Abiera, 1991). The backfill materials were taken from Bangpain Industrial Estate, about 50 km north of Bangkok, Thailand. The index properties of the soil are given in Table 1. The soil specimens for strength tests were compacted at the dry side of optimum to 95° of standard Proctor compaction with a water content of 16%, corresponding to the soil condition used in the large-scale direct shear and pullout tests. The strength parameters were determined from an unconsolidated undrained triaxial test, with a soil sample 102 mm (4 in.) in diameter and 204 mm (8 in.) in height. The cohesion was 57 kPa and the friction angle 35·9°. As mentioned previously, three types of reinforcement materials were used, namely: steel grids, Tensar geogrids, and bamboo grids. For each type of reinforcement material, two grid configurations were selected to enable the influence of the reinforcement geometry on the soil/reinforcement-interaction behavior to be studied. In addition, pullout tests were also made on reinforcements

Table 1
Index Properties of Weathered Bangkok Clay

Natural water content (%)	43·66
Liquid limit (%)	58·70
Plastic index (%)	48·68
Optimum water content (%)	21·00
Maximum dry density (kN/m^3)	16·00
Percentage passing no. 200	82·94

with only longitudinal members to investigate their contributions to the total pullout resistance. Subsequently, two types of welded steel grid were formed by using bars of 6·3 mm (1/4 in.) and 12·7 mm (1/2 in.) diameter with four longitudinal bars equally spaced at 152 mm (6 in.) on centers and six transverse bars evenly spaced at 225 mm (9 in.) on centers. Tensar SS2 and SR80 were used for polymer geogrids, in which the test specimens were cut to 0·45 m in width and 1·2 m in length. The two types of bamboo grid were formed by cutting the bamboo into two sizes, 10 mm by 20 mm and 10 mm by 40 mm in cross-section, and tying together with eight steel wires. The bamboo grids were also constructed with four longitudinal members spaced 152 mm (6 in.) on centers and five transverse members spaced 225 mm (9 in.) on centers. A yellowish to slightly greenish-coloured bamboo specimen was used, which is a very common and cheap species (*Thyrsotachys Oleveri*) found in Thailand.

3.1 The pullout box

The laboratory pullout box was described in detail by Shivashankar (1991). It was built by using 12·7 mm thick (1/2 in. thick) steel plates reinforced with steel beams, and with inside dimensions of 1·27 m × 0·76 m × 0.51 m (50 in. × 30 in. × 20 in.), as shown in Figs 2(a), 2(b). The pullout force was applied by an electro–hydraulically controlled pullout jack through a steel reaction frame. The pullout capacity of this equipment is 22 kN (5000 lbf). The horizontal displacements of the reinforcement were monitored by using a Linear Variable Differential Transformer (LVDT). A data-acquisition system, consisting of an 18-channel micrologger, was employed to record the mat displacement, the pullout forces, and the axial strains in the reinforcements. The rate of pulling was electronically controlled, and a pullout rate of 1 mm/min was adopted. The backfill material was compacted by an impact hand compactor. The density and moisture content of the compacted soil were measured by a nuclear-gage densitometer. The normal pressure was applied by an inflated air bag fitted inside the pullout box over a flexible metal plate, 6.3 mm thick, which was placed directly on top of the compacted backfill soil.

3.2 Large-scale direct-shear devices

A schematic diagram of the large direct-shear apparatus is shown in Fig. 3. Installed on the frame of the pullout-test box, it has a shear area of 0·50 m^2. The same pullout jack was used to apply the shear force. Two 1·24 m long (49 in. long) and 9·5 mm thick (3/8 in. thick) steel channels

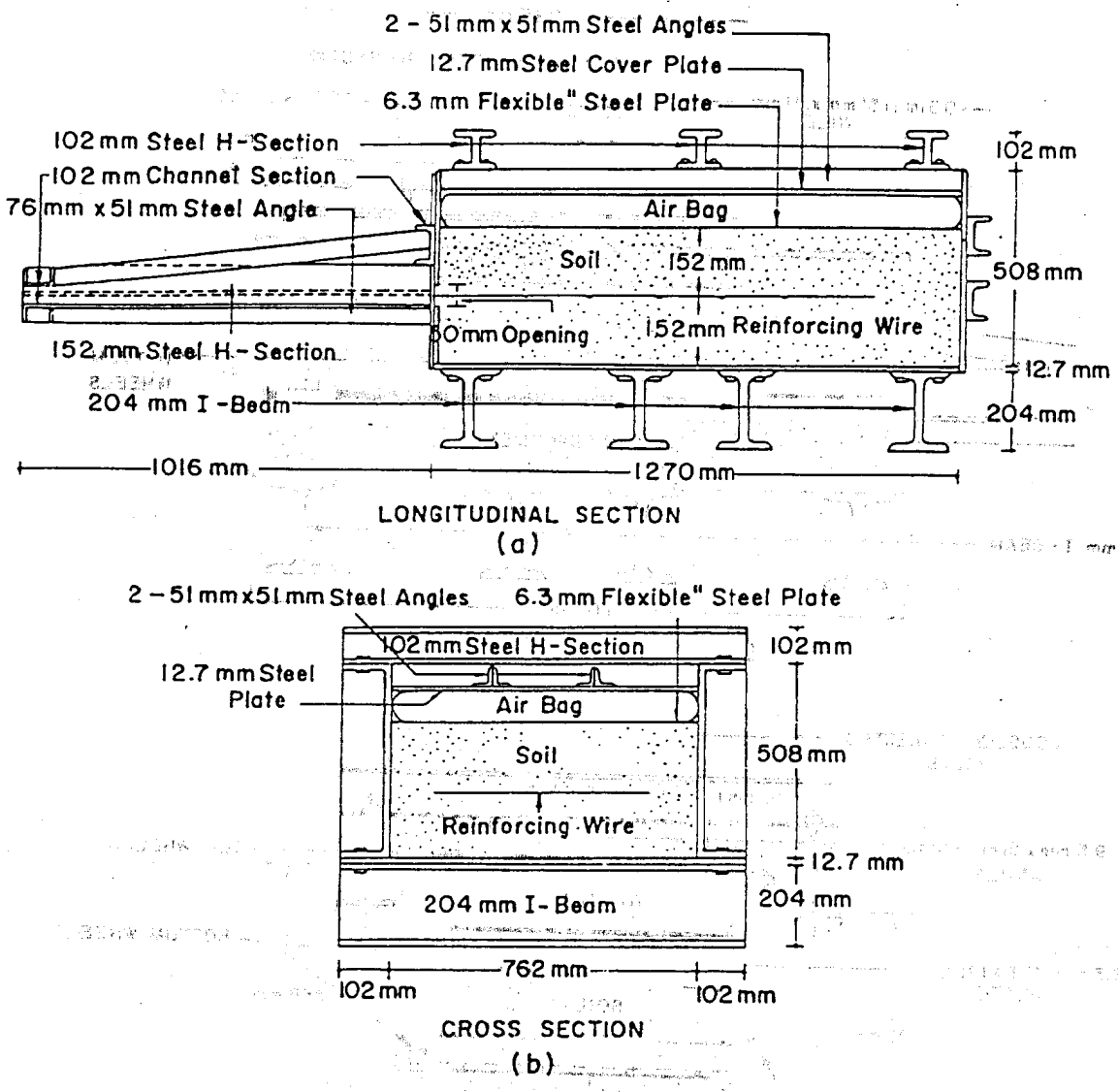

Fig. 2. Pullout box: (a) longitudinal sectional view; (b) cross-sectional view.

(76·2 mm × 152 mm) (3 in. × 6 in.) were placed on both sides at the base of the empty pullout box together with the bottom front plate to form the lower half of the shear box. The upper half of the shear box was made of 9·5 mm thick (3/8 in. thick) steel plate with an inside dimension of 0·94 m (37 in.) in length by 0·58 m (23 in.) in width by 0·56 m (22 in.) in height, which was settled on the two bottom steel channels with roller bearings. Four steel bars, 12·7 mm (1/2 in.) in diameter, were welded in front of the upper box just above a predetermined shear surface so that the shear force could be applied by pulling out the upper-half box. Two steel angle beams and one I-shaped steel beam connected to the pullout box and running along its length formed the reaction frame for the application of normal stress. The top cover was a 6.3 mm thick (1/4 in. thick) steel plate. The roller-bearing system was connected to the reaction frame. The normal

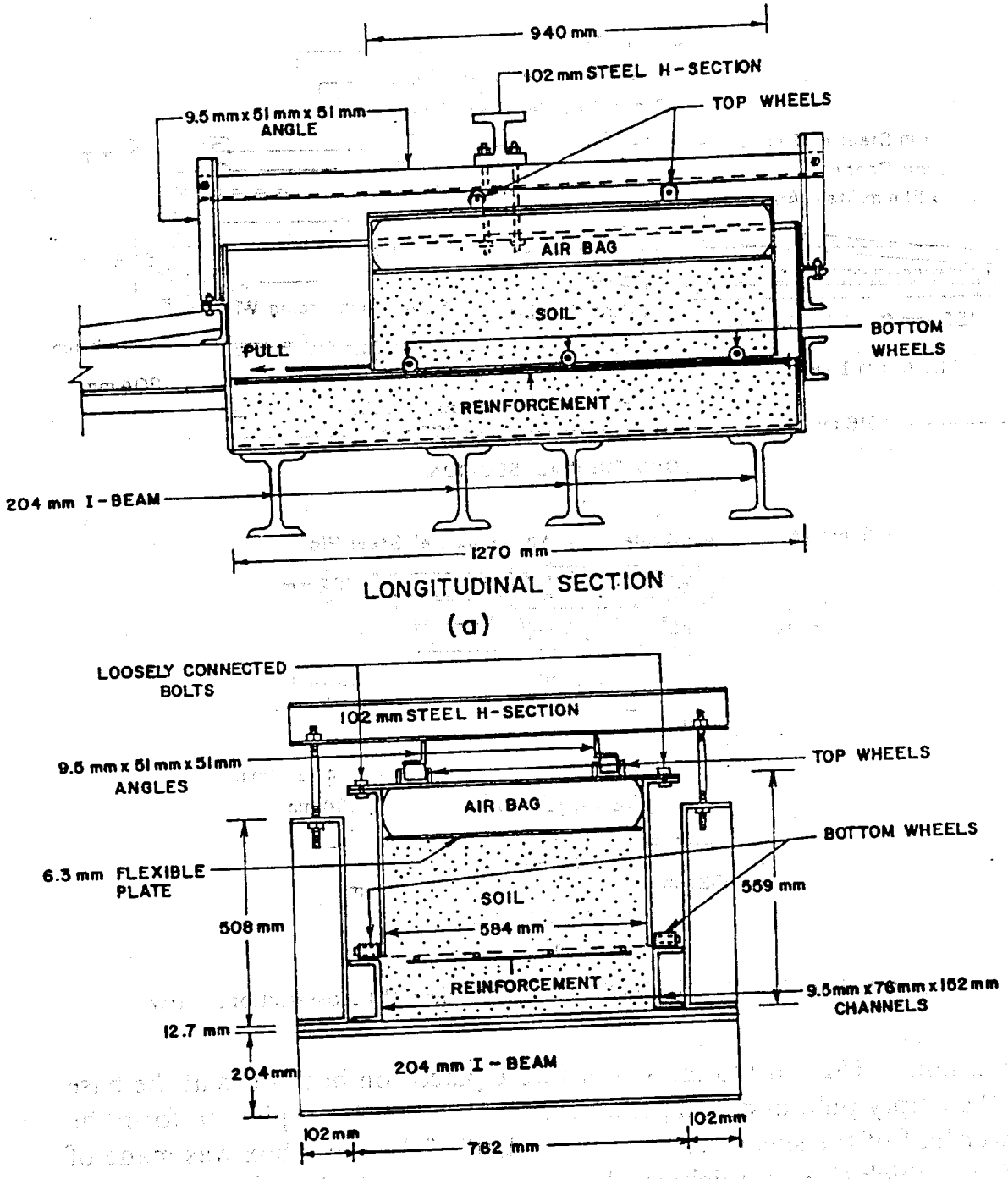

Fig. 3. Large-scale direct-shear box.

pressure was applied by a compressed-air bag. Besides its large shear area, the other advantage of this device is that the inside length of the upper shear box is shorter than that of the lower shear box. Thus, there is no problem of shear-area reduction with the increase in shear displacement.

For the initial set-up of the direct-shear test apparatus, the reinforcement was first fixed at the back end of the lower-half shear box by clamps, and the lower portion of the shear box was filled with compacted soil. The geogrid was then positioned on the soil surface in such a way that it flushed with the predetermined shear surface. The remaining steps are the same as in the conventional direct-shear test.

3.3 Test procedures

For both pullout and direct-shear tests, the multistage procedure was used. First, the low normal pressure was applied. After 25 mm (1 in.) pullout or shear displacement, the test was stopped for 2 hours. The test was then continued under an increased applied normal pressure. For a steel grid, at 25 mm relative displacement, the maximum pullout or direct-shear resistance can be mobilized. Three pullout tests were done in each set-up. The applied normal pressures for each of the three series were: 10, 30, 50; 50, 70, 90; and 90, 110, 130 kPa, respectively. Four large-scale direct-shear tests were made in each set-up with applied normal pressures of 10, 50, 90, 130 kPa. The pullout rate and direct-shear rate of 1 mm/min were adopted for all tests. The measured backfill-soil water content was $16 \pm 0{\cdot}8\%$, and the degree of compaction was 95 ± 2 (dry density of $15{\cdot}2 \pm 0{\cdot}3$ kN/m^3) of standard Proctor compaction.

4 PULLOUT-TEST RESULTS

Figures 4–6 show typical pullout-resistance curves for steel, bamboo, and polymer grids, respectively, at applied normal pressures of 10, 50, and 90 kPa. It is clearly shown that, for inextensible steel and bamboo grids, the resistance mobilization is much faster than that of extensible Tensar SR80 geogrids. As shown in Figs 4 and 5, at a pullout displacement of 25 mm, for steel and bamboo grids either the pullout resistances are fully mobilized or the rate of increase is significantly reduced because the whole grid reinforcement moved nearly as a rigid body (Bergado *et al.*, 1992). However, for Tensar SR80 geogrid, the resistance increased very slowly owing to its extensibility (Fig. 6). Thus, the resistance was mobilized gradually along the embedded reinforcement length. Consequently, in the latter case, the maximum pullout resistance achieved in the test is controlled by the stiffness of the grid reinforcement.

Figure 7 shows plots of the typical measured axial strain versus pullout displacement of steel grid with 6·3 mm bar diameter and 152 mm by 225 mm mesh size. The locations of strain gages are shown in the figure by

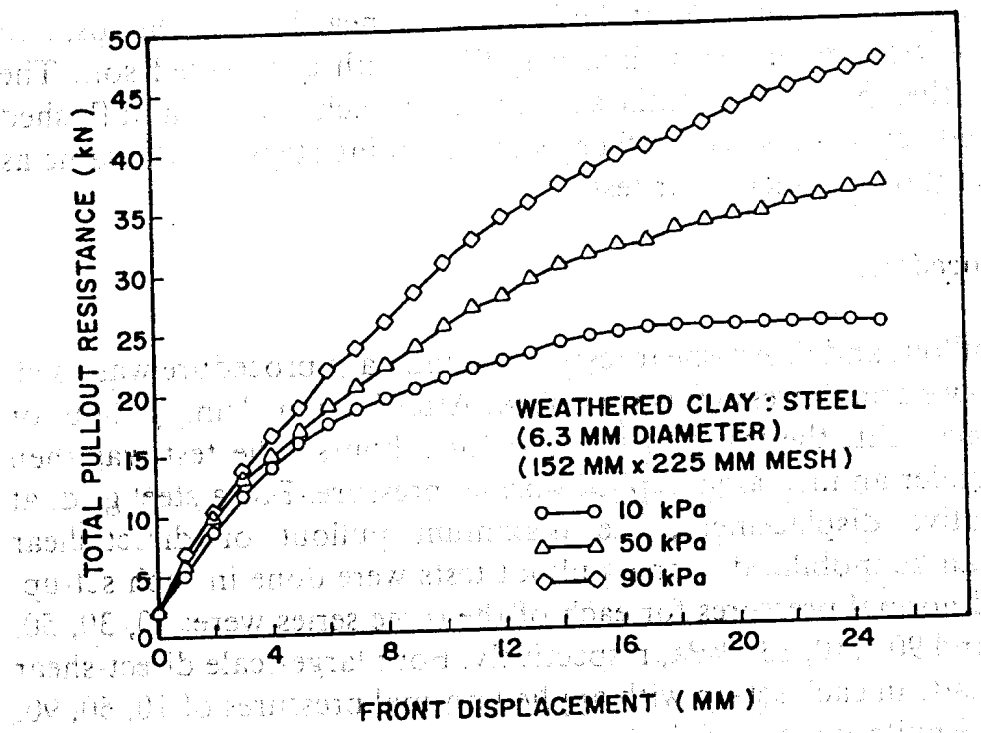

Fig. 4. Pullout-resistance curves for steel grid (6·3 mm bar diameter, 152 mm × 225 mm mesh).

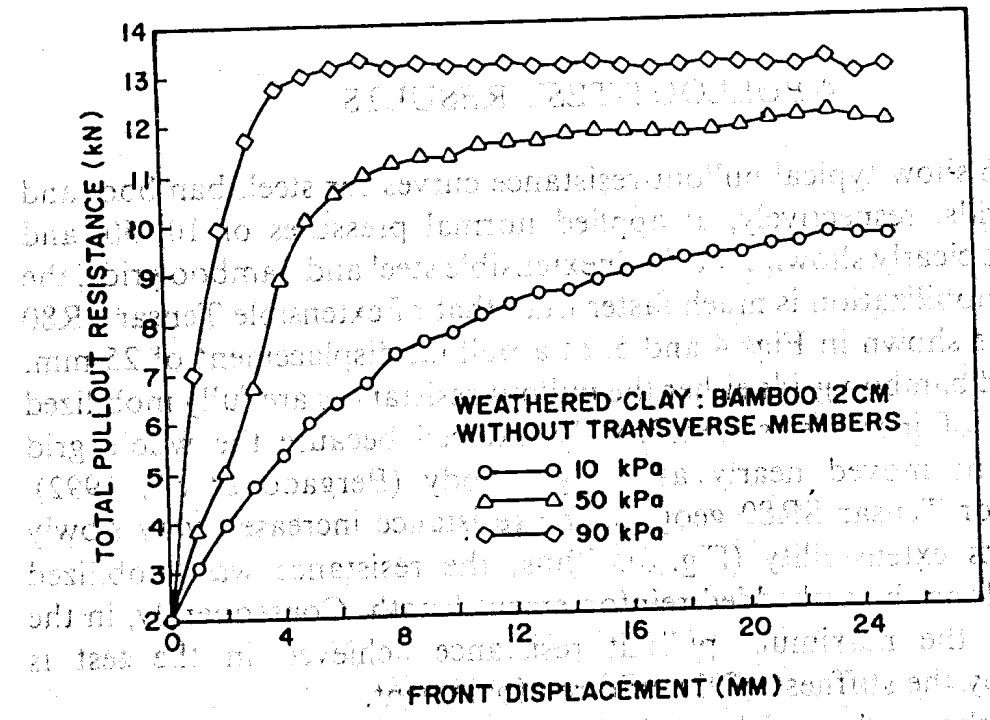

Fig. 5. Pullout-resistance curves for bamboo grid (20 mm bar width, 152 mm × 225 mm mesh).

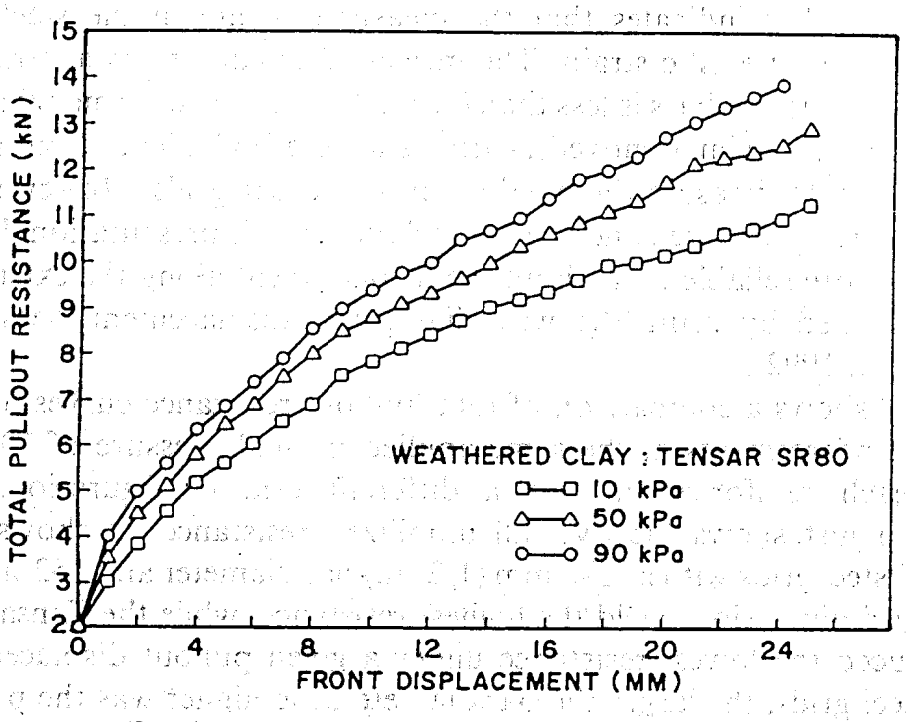

Fig. 6. Pullout-resistance curves for Tensar SR80.

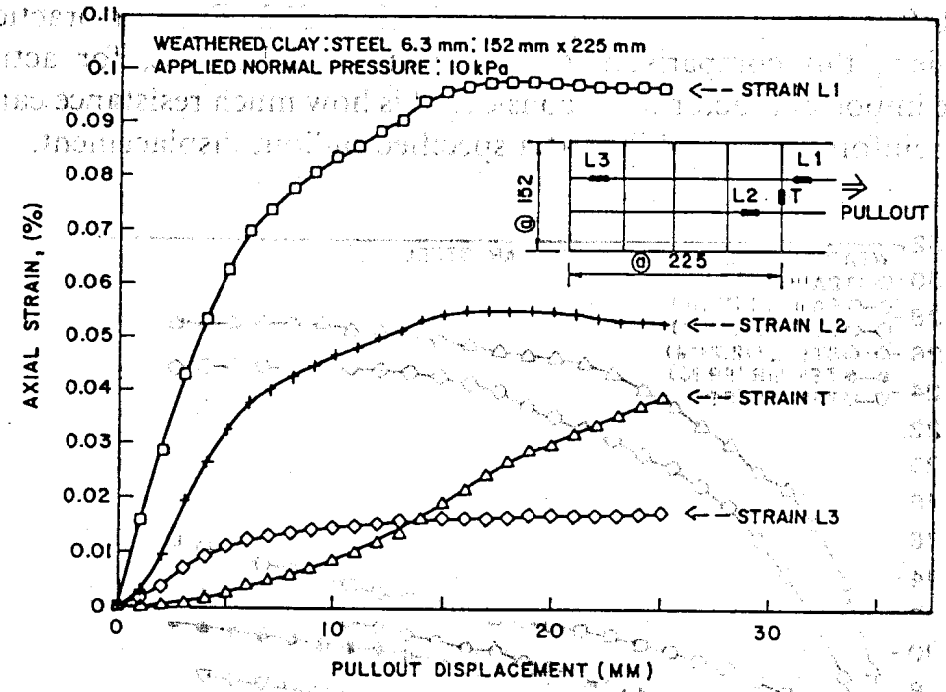

Fig. 7. Typical curves of axial strain versus pullout displacement.

a key sketch, and the applied normal pressure during the test was 10 kPa. It can be seen that the strain in the grid longitudinal bar varies, with the largest value at the location where the pullout force is applied. The shape of the curve of the axial strain in the grid longitudinal bar versus the pullout displacement is similar to that of the curve of pullout force versus pullout

displacement. This indicates that the measured strain in the steel grid longitudinal bar is elastic strain. The measured maximum axial strain in steel-grid longitudinal bars is less than 0·2%. This result confirmed that the whole steel-grid specimen moved nearly as a rigid body. The strain gages were also used to measure the axial strain in Tensar grids. However, the results were quite scattered and are not included in this presentation. It was found that more reliable data about the displacement along the extensible can be obtained by using the wire–dial gauge displacement-measuring system (Chai, 1992).

Figure 8 shows a comparison of total-pullout-resistance curves for the different reinforcements at the same applied normal pressure of 10 kPa. Because each reinforcement has a different grid configuration, this comparison just shows the over-all mobilized resistance. It shows that the welded steel grids with a 12·7 mm (1/2 in.) bar diameter and 152 mm by 225 mm grid dimensions yield the highest resistance, while the Tensar SS2 grid produced the lowest resistance under a given pullout displacement. For the steel grids, the larger the bar diameter, the higher was the pullout resistance for the same grid size. For bamboo grids, the grid with 40 mm width resulted in a higher pullout resistance than that of 20 mm width. Tensar SR80 is stronger and less extensible than SS2. From a practical point of view, this comparison is also meaningful because, for actual design, one important factor to be considered is how much resistance can a particular reinforcement mobilize at a specified pullout displacement.

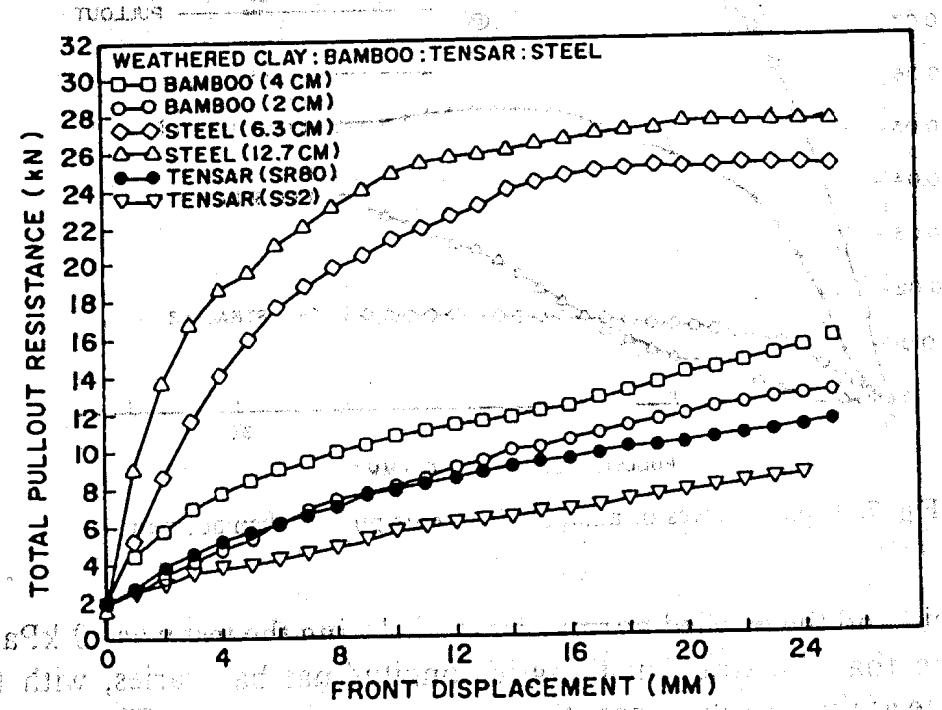

Fig. 8. Comparison of pullout-resistance curves for bamboo, Tensar, and steel grids at 10-kPa applied normal pressure.

Figure 9 plots the total pullout resistance at 25-mm displacement versus the applied normal pressure. The total pullout resistance increased with an increase in the applied normal pressure. However, the increase rate is different for different reinforcement types. The steel grids have a higher rate of increase than the polymer grids and bamboo grids. For extensible reinforcements under a given pullout displacement, the higher the applied normal pressure, the shorter is the length of reinforcement in tension (Ochiai *et al.*, 1988).

The pullout test with only longitudinal members was also conducted to study the frictional component of the pullout resistance. For steel grids, as reported by Bergado *et al.* (1992), the frictional resistance from the longitudinal members was only about 10% of the total pullout resistance, and it was mobilized at a small pullout displacement. Similarly, the transverse members of the Tensar geogrid were also cut away to form the test specimens. All the samples had the same number of longitudinal members as the grid with transverse members. Figure 10 shows the pullout-test results of bamboo and Tensar grids without transverse members at 10-kPa applied pressure. The shapes of pullout-resistance curves are similar to those of the grids with transverse members. A comparison was made of the total pullout resistance of the reinforcement with and without transverse members for bamboo and Tensar grids. A typical plot showing the comparison of the total pullout resistance for Tensar SR80 with and

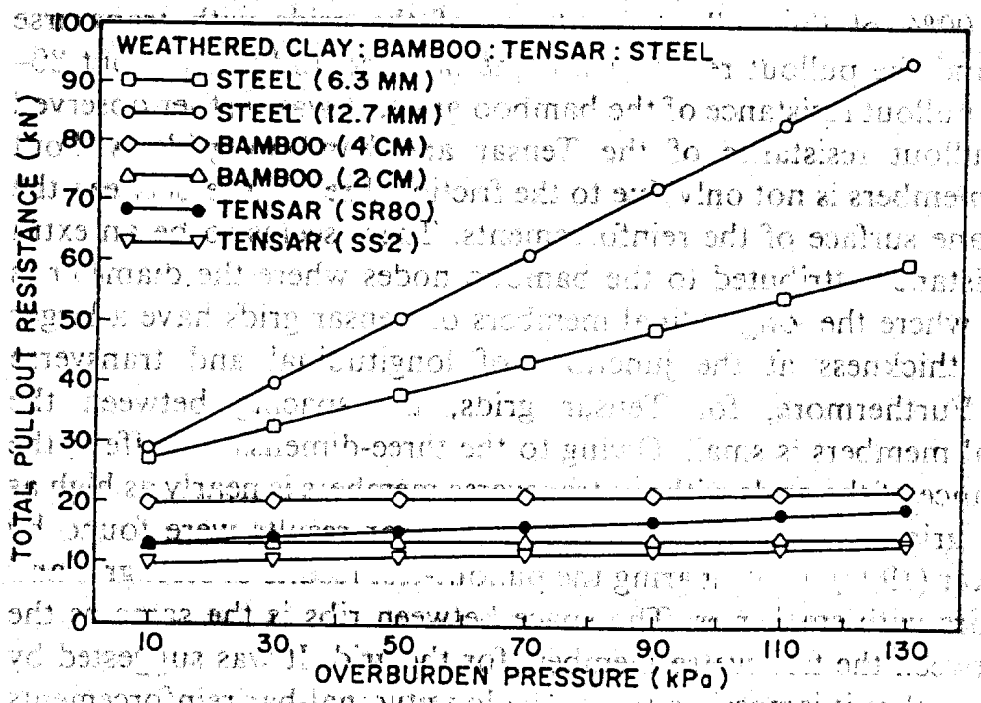

Fig. 9. Comparison of total pullout capacity of bamboo, Tensar, and steel grids at 25 mm pullout displacement.

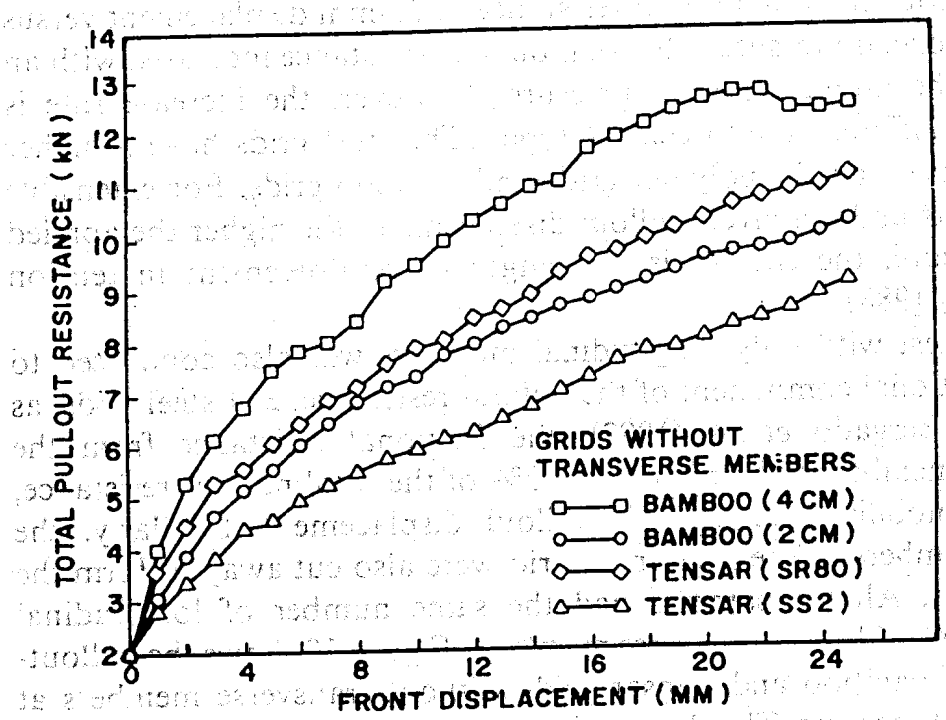

Fig. 10. Pullout-resistance curves for bamboo and Tensar grids without transverse members at 10 kPa applied normal pressure.

without transverse members is illustrated in Fig. 11. It was found that the pullout resistance of Tensar geogrids without transverse members was about 90–100% of the pullout resistance of the grids with transverse members, and the pullout resistance of the bamboo rods was about 80–90% of the pullout resistance of the bamboo grids. It was further observed that the pullout resistance of the Tensar and bamboo grids without transverse members is not only due to the frictional resistance between the soil and plane surface of the reinforcements. There seems to be an extra pullout resistance attributed to the bamboo nodes where the diameter is larger, and where the longitudinal members of Tensar grids have a larger width and thickness at the junctions of longitudinal and transverse members. Furthermore, for Tensar grids, the spacing between the longitudinal members is small. Owing to the three-dimensional effect, the total resistance of the grids without transverse members is nearly as high as that of the grid with transverse members. Similar results were found by Shivashankar (1991) by comparing the pullout-test results of steel grid and the steel bars with small ribs. The space between ribs is the same as the spacing between the transverse members for the grid. It was suggested by Shivashankar that it is possible to use the longitudinal-bar reinforcements only, but with ribs.

The bond coefficient is the parameter that expresses the efficiency of the

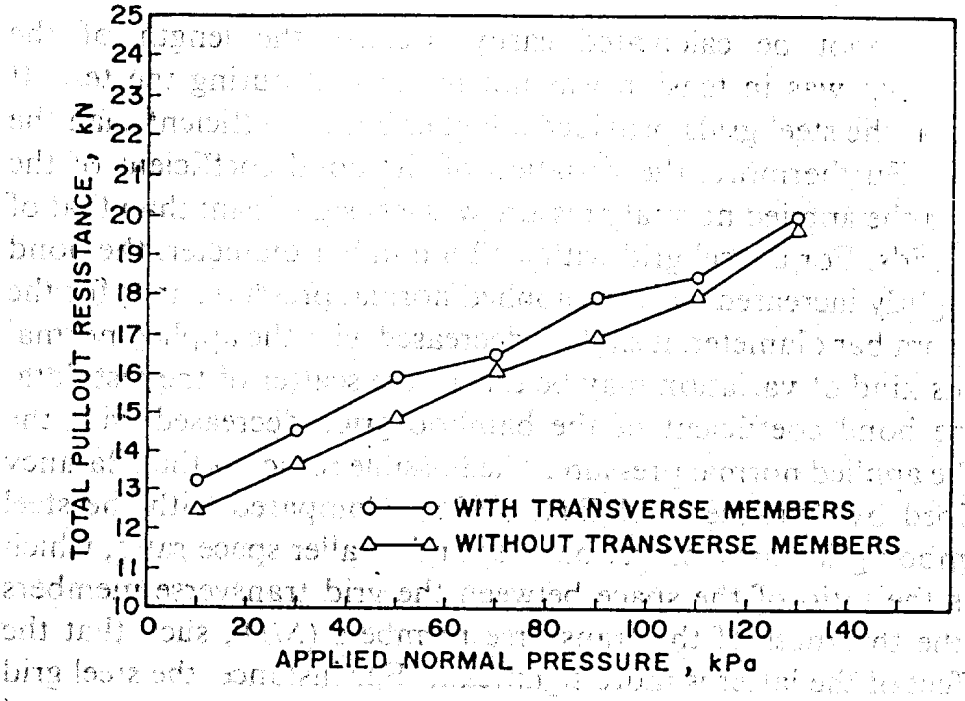

Fig. 11. Comparison of pullout resistance at 25 mm pullout displacement of Tensar SR80 geogrid with and without transverse members.

different grid reinforcements for providing pullout resistance. Figure 12 shows the bond coefficient for steel grids and bamboo grids used in this study. The bond coefficient is calculated using eqn (6) and by using the soil strength parameters from UU-test results. The bond coefficient of the

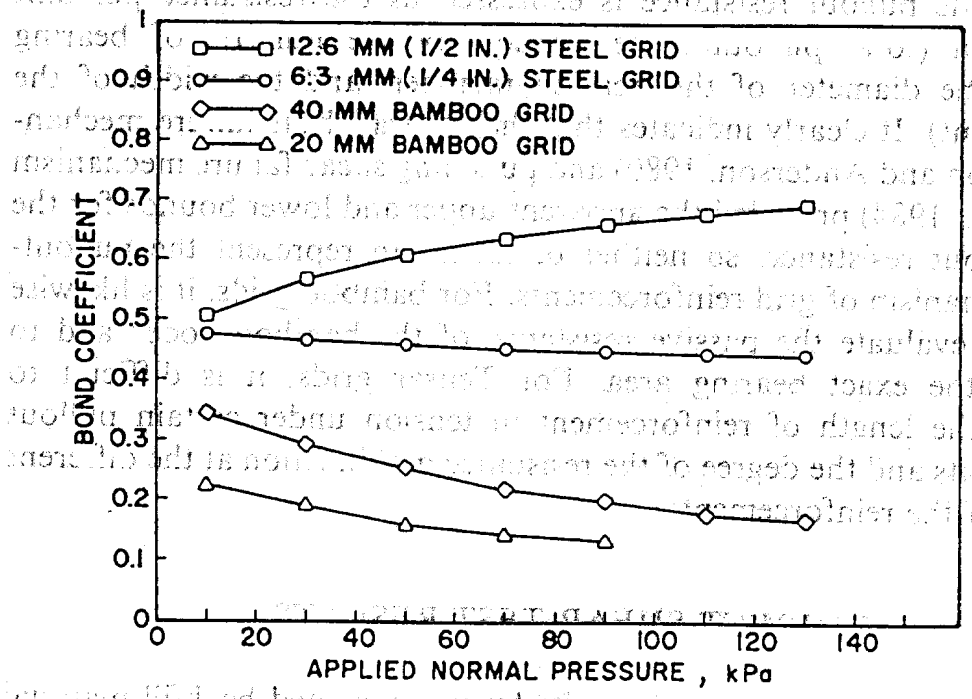

Fig. 12. Bond coefficient for steel and bamboo grids obtained from pullout tests.

Tensar grids cannot be calculated easily because the length of the reinforcement that was in tension was not monitored during the test. It can be seen that the steel grids provided a higher bond coefficient than the bamboo grids. Furthermore, the variation of the bond coefficient of the steel grids with the applied normal pressure was less significant than that of the bamboo grids. For a steel grid with a 12·6 mm bar diameter, the bond coefficient slightly increased with the applied normal pressure, and, for the case of a 6·3 mm bar diameter, it slightly decreased with the applied normal pressure. This kind of variation may be due to the scatter of the test data. However, the bond coefficient of the bamboo grids decreased with the increase in the applied normal pressure. The possible reason is the dilatancy effect described by Schlosser and Elias (1978). Compared with the steel grid, the bamboo grids have bigger bar size and smaller space ratio, which is defined as the ratio of the space between the grid transverse members divided by the thickness of the transverse members (S/D), such that the dilatancy effect of the latter is more significant. For instance, the steel grid with the bar diameter of 12·7 mm (1/2 in.) has twice the bearing area and friction area of the steel grid with a 6·3 mm (1/4 in.) bar diameter, but the bond coefficient of the former is not twice that of the latter. This is attributed to their different space ratios. For the same bearing area, the higher the space ratio, the higher is the pullout resistance (Palmeira and Milligan, 1989). The results of bamboo grids show a similar tendency.

Figure 13 plots the comparison of the calculated and measured maximum total pullout resistance for steel grids with a 6·3 mm bar diameter. The pullout resistance is expressed as the resistance per unit bearing area (total pullout force divided by the number of bearing members, the diameter of the bearing member, and the width of the reinforcement). It clearly indicates that the general shear-failure mechanism (Peterson and Anderson, 1980) and punching shear-failure mechanism (Jewell *et al.*, 1984) provided the apparent upper and lower bounds for the actual pullout resistance, so neither of them can represent the pullout-failure mechanism of grid reinforcements. For bamboo grids, it is likewise difficult to evaluate the passive resistance of the bamboo nodes and to determine the exact bearing area. For Tensar grids, it is difficult to determine the length of reinforcement in tension under certain pullout displacements and the degree of the resistance mobilization at the different positions of the reinforcement.

5 DIRECT-SHEAR-TEST RESULTS

The large-scale direct-shear-test results from compacted backfill material without reinforcement are shown in Fig. 14. The cohesion and friction

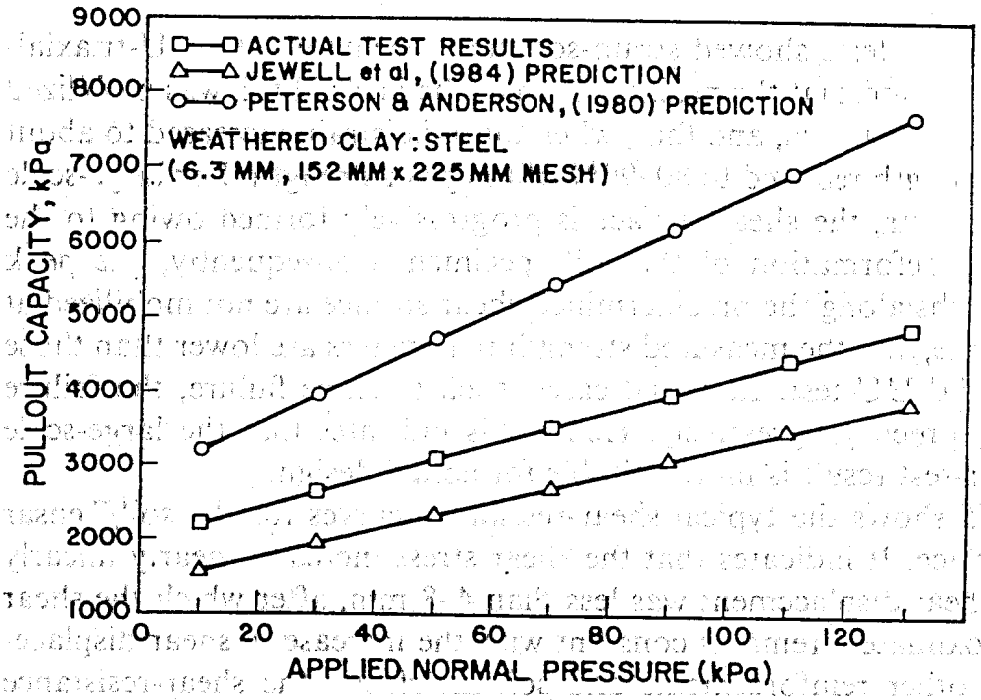

Fig. 13. Comparison of the calculated and measured maximum total pullout resistance for a steel grid with 6·3 mm bar diameter.

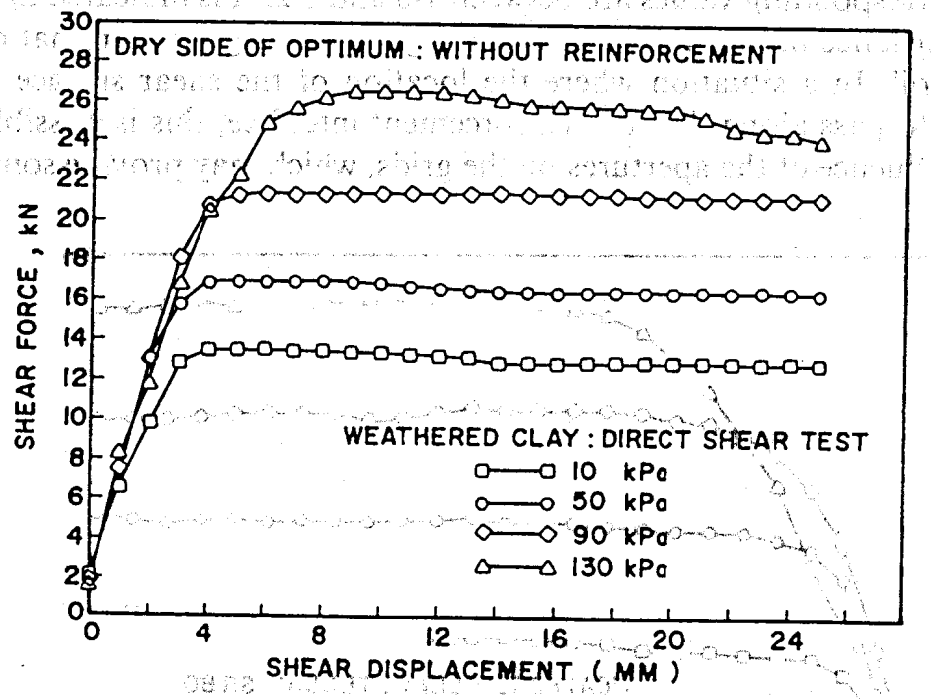

Fig. 14. Large-scale direct-shear-resistance curves for compacted backfill material.

angle were found to be 21·9 kPa and 11·3°, respectively, which are substantially lower than the UU-triaxial-test results. Except for the different shear mechanisms involved in direct-shear and triaxial tests, the main reason for the discrepancy is that the compacted weathered Bangkok

clay used in the tests showed strain-softening behavior. The UU-triaxial-test results showed that the peak strength of the backfill soil was mobilized with 2–4% axial strains, and that, when the axial strain increased to about 10%, the strength reduced to 80–90% of the peak strength. For large-scale direct-shear tests, the shear surface is progressively formed owing to the compressive deformation of the soil specimen. Consequently, the peak shear strengths along the predetermined shear surface are not mobilized at the same time, and the measured strength parameters are lower than those of the triaxial UU test. In actual cases, such as slope failure, the failure surface is formed progressively. Hence this indicates that the large-scale direct-shear-test result is more suitable for actual design.

Figure 15 shows the typical shear-resistance curves for the soil/Tensar SR80 interface. It indicates that the shear stress increased nearly linearly when the shear displacement was less than 4–8 mm, after which the shear force approximately remains constant with the increase in shear displacement. For other reinforcements and soil interfaces, the shear-resistance curves have a similar shape to that in Fig. 15.

Figure 16 shows the bond coefficients of Tensar grids from direct-shear tests. The corresponding values are between 1·0 and 1·2. It is indicated that the shear resistance between the soil and the grids was higher than that of the soil to soil. In a situation where the location of the shear surface is constrained to pass along the soil-reinforcement interface, this is possibly due to the influence of the apertures on the grids, which may provide some

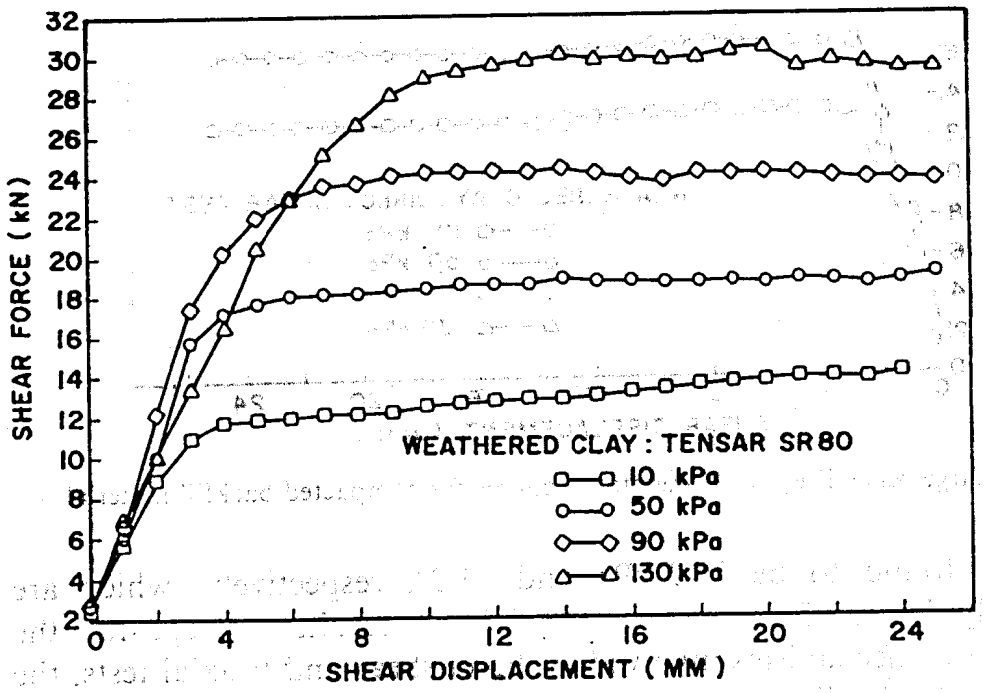

Fig. 15. Large-scale direct-shear-resistance curves for Tensar SR80/soil interface.

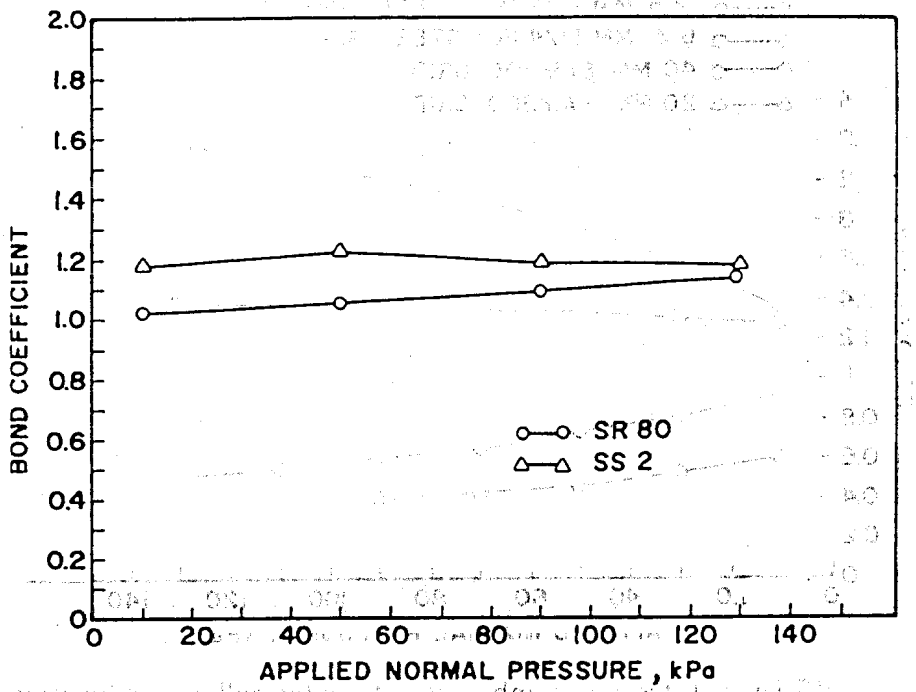

Fig. 16. The bond coefficient of Tensar geogrids from large-scale direct-shear tests.

amount of bearing resistance during shear. However, it is difficult to measure the bearing effect of the apertures on the grids quantitatively. In the field, the shear plane will pass through the plane with lowest resistance, so that the bond coefficient cannot exceed unity. These results indicate that the soil/grid reinforcement interface can provide the same shear strength as the soil itself.

Figure 17 shows the bond coefficients of steel and bamboo grids obtained by using the soil-strength parameters from large-scale direct-shear test. It shows that the bond coefficients of the steel grids are larger than 1·0, whereas, for bamboo grids, the corresponding values are smaller than 1·0. Comparing this observation with the results in Fig. 12 shows that using the soil-strength parameters from the large-scale direct-shear test yields a higher bond coefficient than that obtained by using the triaxial-test soil-strength parameters. The estimation of bond coefficient therefore depends on the kind of test used to determine the soil-strength parameters that are used for calculation.

6 CONCLUSIONS

Large-scale laboratory pullout and direct-shear tests were employed to investigate the interaction properties between weathered Bangkok clay and various reinforcements, consisting of steel grids, bamboo grids, and Tensar

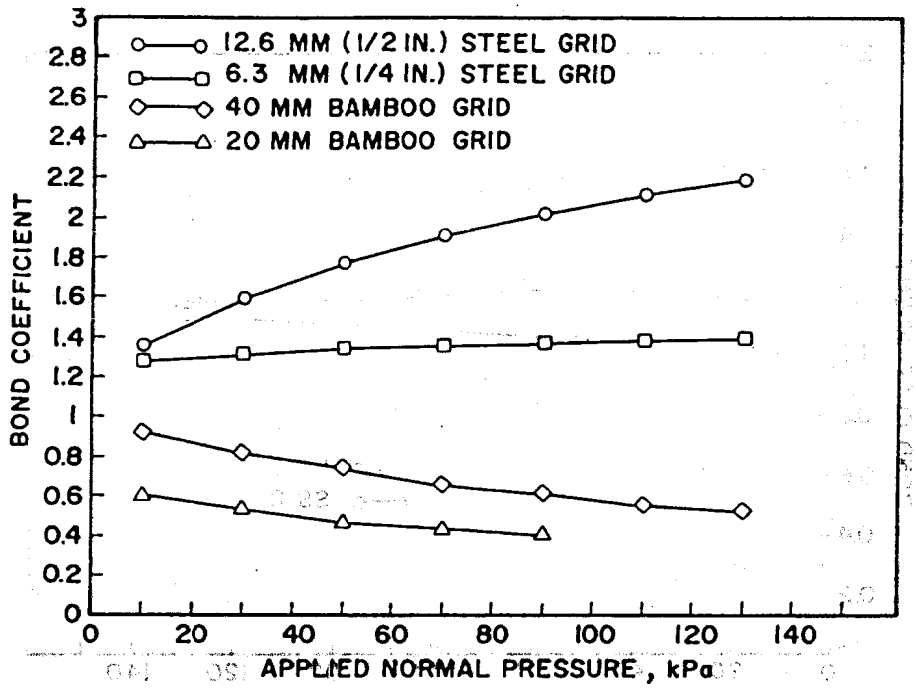

Fig. 17. Bond coefficients of steel and bamboo grids from the pullout test by using the soil-strength parameters from large-scale direct-shear tests.

SR80 and SS2. On the basis of the test results, the following conclusions can be drawn.

(1) During the pullout test, for inextensible reinforcements, such as steel and bamboo grids, the whole grids move approximately as a rigid body, the resistance mobilized uniformly along the reinforcement, and the total pullout resistance can reach the maximum value under a relatively small pullout displacement. However, for extensible reinforcements, such as polymer grids, the elongation of the reinforcement varied non-linearly along the reinforcement length, which resulted in non-uniform resistance mobilization, and thus the maximum pullout resistance achieved is controlled by the stiffness of the reinforcement.

(2) For steel grids, about 90% of the pullout resistance is derived from the passive-bearing resistance of transverse members. For bamboo and Tensar grids, owing to the influence of the nodes or ribs on the longitudinal members, the pullout resistance of the grids without transverse members proved to be 80–90% of that of the grids with transverse members.

(3) The steel grids yielded a higher bond coefficient than that of the bamboo grids. The decrease in the bond coefficient for bamboo grids is possibly due to the dilatancy effect of the backfill soil. The bond

coefficient of the Tensar grids in a pullout test cannot be easily calculated because of the variation in the degree of pullout-resistance mobilization along the reinforcement.

(4) For inextensible reinforcements, the general shear-failure mode and punching shear-failure mode provide apparent upper and lower bounds, respectively, of the pullout-test results.

(5) The large-scale direct-shear strength of the weathered clay was much lower than the triaxial-test results. Besides the different shear mechanisms of these two types of test, for the case of the large-scale direct-shear test, the shear plane is formed progressively, and the strength parameters obtained may not represent the peak strength of the soil.

(6) Owing to the influence of the apertures on the grid reinforcements, the shear resistance between the grids and the soil in a direct-shear test can be equal to or larger than the shear resistance between soil and soil.

REFERENCES

Abiera, H. O. (1991). Mechanically stabilized earth using Tensar, bamboo and steel grid reinforcements with weathered Bangkok clay as backfill. M. Eng. thesis, No. GT-90-21, Asian Institute of Technology, Bangkok, Thailand.

Bergado, D. T., Sampaco, C. L., Shivashankar, R., Alfaro, M. C., Anderson, L. R. & Balasubramaniam, A. S. (1991). Performance of a welded wire wall with poor quality backfills on soft clay. In *Proceedings of ASCE 1991 Geotechnical Engineering Congress, Boulder, CO, USA*, ed. F. G. McLean, D. A. Campbell & D. W. Harris. ASCE Geotechnical Special Publication No. 27, pp. 908–22.

Bergado, D. T., Hardiyatimo, H. C., Cisneros, C. B., Chai, J. C. Alfaro, M. C. & Anderson, L. R. (1992). Pullout resistance of steel geogrid with weathered clay backfill material. *Geotech. Testing J.*, **15**(1), 33–46.

Bergado, D. T., Lo, K. H., Chai, J. C., Shivashankar, R., Alfaro, M. C. & Anderson, L. R. (1992). Pullout tests using steel grid reinforcement with low quality backfill. *J. Geotech. Engng. Div., ASCE*, **118**(7), 1047–63.

Chai, J. C. (1992). Interaction between grid reinforcement and cohesive-frictional soil and performance of reinforced wall/embankment on soft ground. D. Eng. dissertation, Asian Institute of Technology, Bangkok, Thailand.

Chang, J. C., Hannon, J. B. & Forsyth, R. A. (1977). Pull resistance and interaction of earthwork reinforcement and soil. *Transportation Res. Rec.*, **640**, 1–7.

Jewell, R. A., Milligan, G. W. E., Sarsby, R. W. and Dubois, D. (1984). Interaction between soil and geogrids. In *Proceedings of Symposium on Polymer Grid Reinforcement*. Thomas Telford Ltd, London, pp. 18–29.

Ochiai, H., Hayashi, S., Othni, J., Umezaki, T. & Ogisako, E. (1988). Field pullout test of polymer grid in embankment. In *Proceedings of the International*

Symposium on Theory and Practice of Earth Reinforcement, Fukuoka, Japan, ed. T. Yamanouchi, N. Miura & H. Ochiai. A.A. Balkema, Rotterdam, pp. 147–51.

Palmeira, E. M. & Milligan, G. W. E. (1989). Scale and other factors affecting the results of pullout tests of grids buried in sand. *Geotechnique,* **39**, 511–24.

Peterson, L. M. & Anderson, L. R. (1980). Pullout resistance of welded wire mesh embedded in soil. Research report submitted to Hilfiker Pipe Co., Department of Civil Engineering, Utah State University, Logan, UT, USA.

Schlosser, F. & Elias, V. (1978). Friction in reinforced earth. Paper presented at Symposium on Earth Reinforcement, ASCE Annual Convention, Pittsburgh, PA, USA.

Shivashankar, R. (1991). Behavior of a mechanically stabilized earth (MSE) embankment with poor quality backfills on soft clay deposits, including a study of the pullout resistances. D. Eng. dissertation, Asian Institute of Technology, Bangkok, Thailand, (1991).